Numerical Study of Microstructural Evolution of IN625 During Pulsed Laser Welding

Paper ID: 137

Rakibul Islam Kanak[1] Badhon Kumar[1]

[1]Department of Mechanical Engineering
Bangladesh University of Engineering and Technology

15th International Conference on Mechanical Engineering (ICME) 2025
December 17-18, 2025
BUET, Dhaka, Bangladesh

Outline

Introduction

Laser Welding

One of the most preferred welding techniques due to excellent precision and high energy density – produces excellent quality joints.

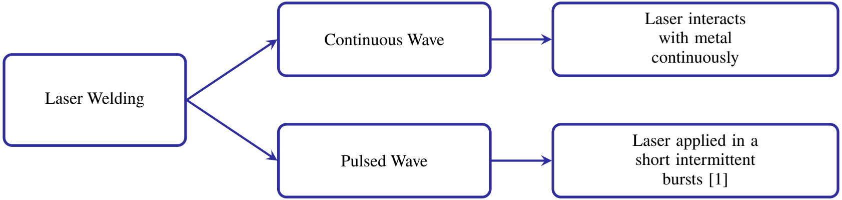

Our Work

Why Pulsed Laser Welding?

- Enhanced control of heat input and melt pool dynamics [3]
- Precise control of cooling rate and grain structure [5]

Why Nickel-Based Superalloys?

- Superior strength-to-weight ratio
- Exceptional resistance to creep, corrosion, and high temperatures [6]

Research Gap

- Experimental parametric studies are cost-prohibitive and time-intensive

This Work

- Coupled CFD-CA framework for pulsed laser welding of IN625
- Established predictive process-structure relationships

Mathematical modeling

Thermo-fluid Transport Equation

$$\nabla \cdot (\mathbf{u}) = 0 \tag{1}$$

$$\rho \left[\frac{\partial \mathbf{u}}{\partial t} + \nabla \cdot (\mathbf{u}\mathbf{u}) \right] = \nabla \cdot (\mu \nabla \mathbf{u}) - \nabla p + \rho \beta (T - T_0)\mathbf{g} - \mu \frac{180}{\lambda^2} \frac{f_s^2}{(1 - f_s)^3} \mathbf{u} \tag{2}$$

$$\rho c_p \left[\frac{\partial T}{\partial t} + \nabla \cdot (\mathbf{u} T) \right] = \nabla \cdot (k \nabla T) + \rho L_f \frac{\partial f_s}{\partial t} + Q \tag{3}$$

Gaussian Heat Source

$$Q(x, y, z) = \frac{2\eta P}{r_{xy}^2 d \pi^{3/2}} \exp\left(- \left(\frac{2(x - x_0)^2}{r_{xy}^2} + \frac{2(y - y_0)^2}{r_{xy}^2} + \frac{2(z - z_0)^2}{d^2} \right) \right) \tag{4}$$

Heterogeneous Nucleation

$$f(\Delta T) = \frac{1}{\Delta T_\sigma \sqrt{2\pi}} \exp\left(-\frac{1}{2} \left(\frac{\Delta T_\mu - \Delta T}{\Delta T_\sigma} \right)^2 \right) \tag{5}$$

Model Validation

The numerical model was validated using experimental data from the *NIST Additive Manufacturing Benchmark 2018 Challenge* [4] across 3 distinct welding conditions:

Case	**Power (W)**	**Speed (mm/s)**
A	137.9	400
B	179.2	800
C	179.2	1200

Table: Welding Process Parameters

Validation Metrics

- Melt pool geometry
- Cooling rates
- Microstructure predictions

** NIST AM Bench is an international benchmark series for validating computational models against standardized additive manufacturing experiments.*

Thermo-Fluid Validation

The thermo-fluid model was validated by comparing predicted melt pool dimensions (depth and width) against experimental measurements through qualitative and quantitative analysis.

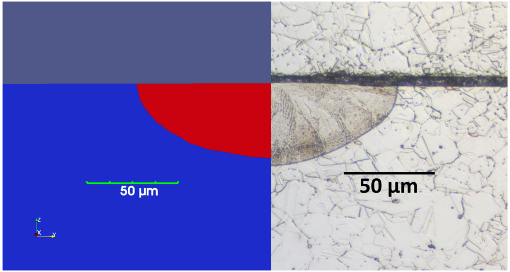

(a) Qualitative comparison of melt pool morphology for case B

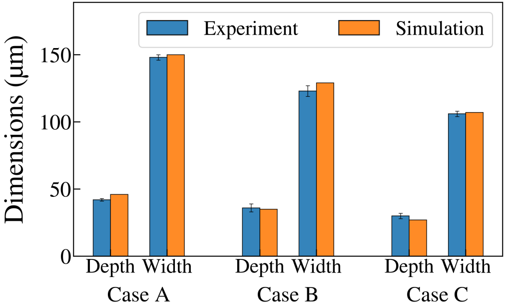

(b) Quantitative validation of melt pool dimensions for all 3 cases

Microstructure Validation

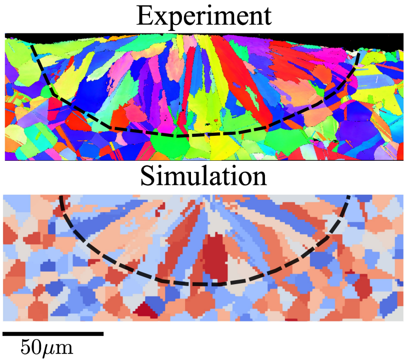

(a) Qualitative comparison of grain structure (Case B)

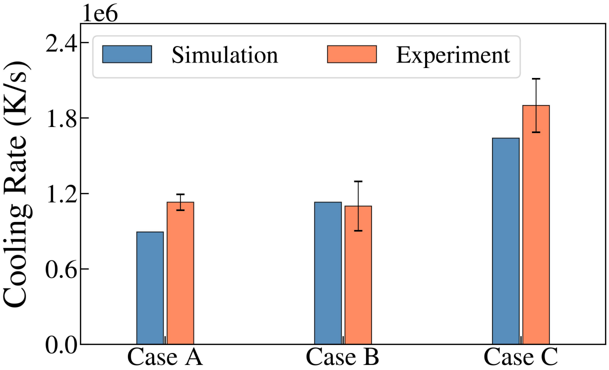

(b) Quantitative validation of grain dimensions

Pulse Laser Setup

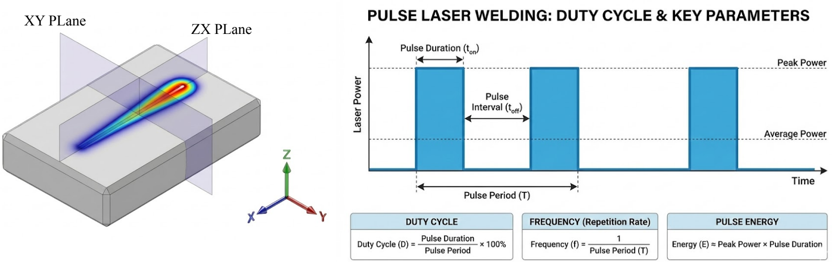

Figure: Illustration of the cross-section taken to analyze the results (left) and terminology of the Pulsed Laser [2] (right)

Pulse Laser Setup

- Four pulsed welding cases: 2, 8, 20, and 50 kHz
- AMMT Case B parameters with 0.5 duty cycle
- Peak power doubled to maintain equivalent average power

Results

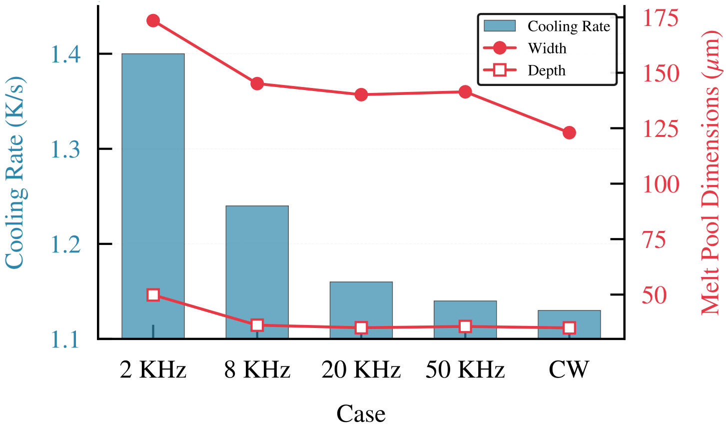

Figure: Melt pool dimensions and cooling rate for PW and CW cases

Results

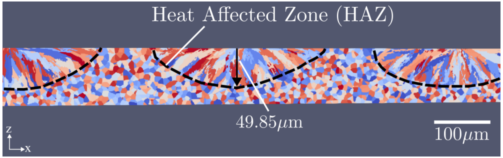

(a) 2 KHZ ZX Plane

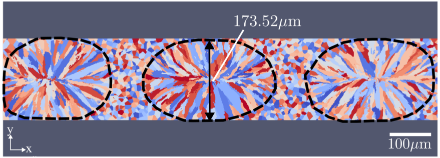

(a) 2 KHZ XY Plane

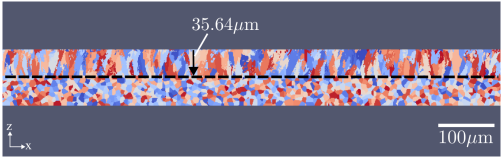

(a) 50 KHZ ZX Plane

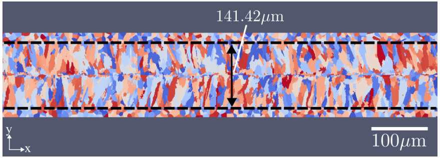

(a) 50 KHZ XY Plane

Figure: Grain textures for 2 and 50 KHz cases in the top plane (XY) and longitudinal section (ZX)

Results

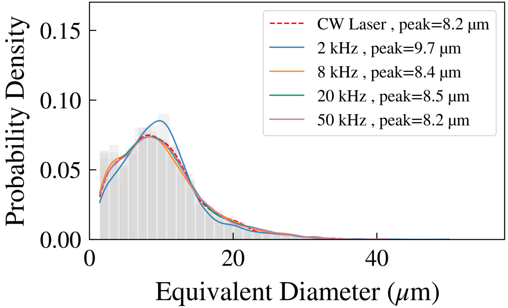

(a) PDF of equivalent grain diameter

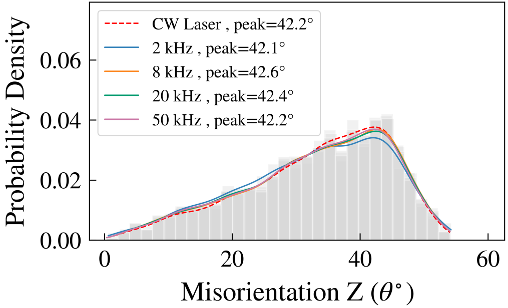

(b) PDF of misorientation angle Z

Figure: Grain Statistics of All 4 cases of Pulse laser welding along with continuous laser

Conclusions

Key Findings

- Established frequency-dependent relationship: cooling rate and grain refinement inversely correlate with pulsing frequency (2–50 kHz)
- Higher frequencies yield finer columnar grains (≈ 8.2 µm)
- Lower frequencies produce coarser grains (≈ 9.7 µm)
- Peak Z-axis misorientation observed at 8 kHz, diminishing at higher frequencies

Significance

- Validated coupled CFD-CA framework against NIST AM-Bench 2018 experimental data
- Demonstrated frequency modulation as effective tool for microstructure control in IN625
- Bridges critical gap in understanding pulsed laser processing of nickel-based superalloys

References I

[1] M. Chludzinski et al. "Pulsed Laser Welding Applied to Metallic Materials—A Material Approach". In: *Metals* 11.4 (2021), p. 640. DOI: 10.3390/met11040640.

[2] GoPhotonics. *What is the Duty Cycle of a Laser?* Accessed: 2025-01-18. 2024. URL: https://www.gophotonics.com/community/what-is-the-duty-cycle-of-a-laser.

[3] C. Guo et al. "A comparing study of defect generation in IN738LC superalloy fabricated by laser powder bed fusion: Continuous-wave mode versus pulsed-wave mode". In: *Journal of Materials Science & Technology* 90 (2021), pp. 45–57. DOI: 10.1016/j.jmst.2021.03.006.

[4] B. Lane et al. "Measurements of Melt Pool Geometry and Cooling Rates of Individual Laser Traces on IN625 Bare Plates". In: *Integrating Materials and Manufacturing Innovation* 9.1 (2020), pp. 16–30. DOI: 10.1007/s40192-020-00169-1.

[5] P. Peyre et al. "Comparison between modulated-pulsed and continuous wave laser powder bed fusion on an Inconel 625 alloy". In: *Progress in Additive Manufacturing* (2025). DOI: 10.1007/s40964-025-01050-3.

[6] G. R. Thellaputta, P. S. Chandra, and C. S. P. Rao. "Machinability of Nickel Based Superalloys: A Review". In: *Materials Today: Proceedings* 4.2 (2017), pp. 3712–3721. DOI: 10.1016/j.matpr.2017.02.266.